Evaluation of two Shielding Strategies

H. Sanchez[1], M. Poole[1], F. Liu[1], and S. Crozier[1]

[1]School of Information Technology & electrical Engineering, The University of Queensland, Brisbane, QLD, Australia

Introduction: During gradient coil operation, eddy-currents (ECs) are induced in nearby conducting metallic structures. These currents generate detrimental transient magnetic fields in the region of interest (ROI) and hence, active and/or passive shielding is required to minimize the consequential image distortion. The first actively-shielded gradient coils [1] constrained the stray field produced by the coil to zero at the cryostat surface. This does not guarantee minimal EC influence within the ROI; an alternate approach is to minimise the EC-induced magnetic field in the ROI directly [2]. A symmetry-free numerical method employing the principle of Equivalent Magnetization Current (EMC) [3] was used in the present study to evaluate these two approaches to gradient coil shielding. This evaluation was made by simulating the ECs generated by coils designed with stray magnetic field minimization (method A) and EC-induced magnetic field minimization (method B). Each gradient coil was driven with a trapezoidal-shaped current pulse and the ECs, along with their effect on the magnetic field in the ROI, were simulated. Moreover the EC-induced fields were decomposed into spherical harmonics to observe their behaviour during and after the trapezoidal pulse. Parameters of coil performance such as efficiency, linearity and figure of merit (FoM) were also calculated to give a full comparison between methods A and B.

Method: In all coils, The EMC approach was employed in the present study as the method of gradient coil design. Cylindrical gradient coils were designed with a primary radius of 344 mm and 1074.4 mm length, whilst a 435 mm radius cylinder of length 1356 mm formed the active shielding surface. A cylindrical cryostat was modelled using a 475 mm radius cylinder of length 1700 mm, on which ECs were induced and their effects simulated. The conductivity of the cryostat surface was assumed to be that of steel and its thickness was 3.18 mm (this thickness simply affects the conductivity of the cryostat and no skin-depth-effects were modelled). The same geometry and coil size, ROI and cryostat surface were employed in all cases. The present implementation of the EMC method of gradient coil design uses quadratic programming (QP) in which the stored energy and/or power dissipation of the coil is minimised subject to linear constraints of field linearity, torque-balancing and the shielding condition. A trapezoidal pulse of 100 μs ramp-up and ramp-down with a flat-top of 400 μs was used to analyse the EC transient behaviour and field contribution in the ROI.

Shielding method A ($|\mathbf{B}^{cryo}| = 0$)**:** Coils designed using method A were shielded by forcing the magnetic field magnitude at an ensemble of points on the cryostat surface to be zero (or as close to zero as possible). This was achieved by including the magnitude of the magnetic field at these points as linear constraints in the QP problem.

Shielding method B ($B_z^{EC} = 0$)**:** Here, the axial component of the magnetic field generated by the induced ECs (B_z^{EC}) is annulled within the ROI. From the work of Peeren [2] it was shown that an "instantaneous" EC is induced when the coil is switched on. The magnetic field produced by the EC is determined by the self-inductance of the cryostat surface ($\mathbf{M}_{cc}$) and the mutual coupling between the coil and the cryostat surface ($\mathbf{M}_{cs}$);

$$B_z^{EC} = -\mathbf{E}\mathbf{M}_{cc}\mathbf{M}_{cs}\boldsymbol{s},$$

where the vector $\boldsymbol{s}$ contains the stream function amplitude at each node on the coil surface and the matrix $\mathbf{E}$ contains the field contribution of the cryostat surface in the ROI. The network approach [2], assuming dissipation, is used to simulate the transient behaviour of the EC at the DSV.

Results and Discussions: Four gradient coils were designed, three of which are shown in Fig. 1. Two of the four coils (one *z*- and one *x*-gradient) were designed using method A and another two coils were designed using method B. Table 1 shows the properties of the gradient coil when 46 contours were used. Coils designed using method B are characterized by a smaller FoM than those of method A. The coil pattern obtained with method B appears to cover more of the shielding surface and hence larger coil resistances and smaller coil efficiencies were exhibited (c.f. Fig.1 (**d** and **g**)). However, the residual gradient produced by method B after the pulse is ramped-up and ramped-down (max/min (G_o^{Eddy})/ G_o^{Coil}·100) is more than 100 times smaller than the same value produced by method A. Figs. 1 (**b**,**e** and **h**) show the transient behaviour of the EC-induced gradient field when the coil is excited with a trapezoidal pulse. The coils designed with method B are likely to require less pulse pre-emphasis compared to those of method A. From Figs. (**c**, **f**, and **i**) it can be seen that the interested magnetic field spherical harmonics generated by the coils designed with method B dissipate faster than those of method A. However, the peak-peak value of the magnetic field at the cryostats is larger in method B than A. The pattern of ECs induced with method B contains high frequency oscillations which dissipate more rapidly. The field from these oscillatory currents somewhat cancel each other out at the ROI.

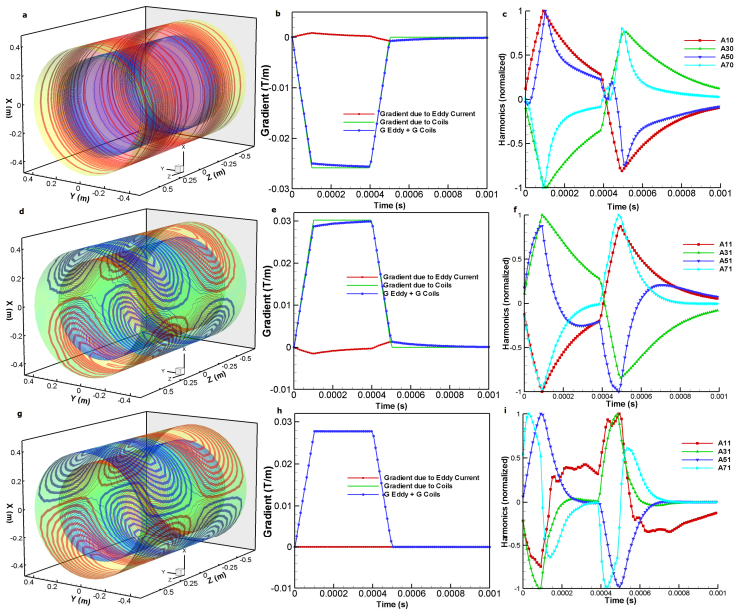

Fig. 1. *Gradient coils designed using different strategy.* (**a**) (**d**) *Shielded z(x)-gradient coil designed with traditional technique* (|**B**|*=0 at the shielding surface*) (**b**,**e**) *The resulting gradient field and the* (**c**,**f**) *normalized harmonic amplitudes vs time.* (**g**) *x-gradient coil designed with method B.* (**h**) *The resulting gradient field and the* (**i**) *normalized harmonic amplitudes vs time.*

Table I. Gradient Coil Properties

Properties-Z	$\lvert(B_z,B_x,B_y,)\rvert^{\text{at screen}} \leq B_z^{\text{Shield}}$	$\lvert B_z^{\text{at DSV}} \rvert \leq B_z^{\text{Shield}}$ Eddy Current Control
Conductor Thickness (mm) (P/S)	4.9/1.8	4.9/1.8
Conductor constant width (mm) (P/S)	4.7/17.8	4.9/17.8
FoM, η /L ($T^{-2}\cdot m^{-2}\cdot A^{2}\cdot H^{-1}$)	$10.65\cdot10^{-6}$	$10.45\cdot10^{-6}$
Coil Resistance (mΩ)	97.12	98.63
Max. field error, ΔB_z^{max} (%)	3.71	3.7
Residual Eddy Current Gradient (%)	2.71	0.023
p-p. magnetic field at cryostats (μT/A)	B_z=3.91, B_x=3.4, B_y=3.7	B_z=10.7, B_x=10.7, B_y=10.5
Properties -X	$\lvert(B_z,B_x,B_y,)\rvert^{\text{at screen}} \leq B_z^{\text{Shield}}$	$\lvert B_z^{\text{at DSV}} \rvert \leq B_z^{\text{Shield}}$ Eddy Current Control
FoM, η /L ($T^{-2}\cdot m^{-2}\cdot A^{2}\cdot H^{-1}$)	$7.01\cdot10^{-6}$	$5.85\cdot10^{-6}$
Coil Resistance (mΩ)	175.9	187.06
Max. field error, ΔB_z^{max} (%)	4.80	4.80
Residual Eddy Current Gradient (%)	4.4	0.012
p-p. magnetic field at cryostats (μT/A)	B_z=7.6, B_x=7.8, B_y=8.5	B_z=15.6, B_x=13.3, B_y=8.7

Conclusions: We have presented an evaluation between two known coil design shielding strategies: annulling of the stray field at the cryostat (method A) and annulling of the EC-induced field in the ROI (method B). Coils designed with method B exhibit slightly reduced FoM than the conventional designs, but appear in simulation to require less pulse pre-emphasis. Moreover, the dominant field harmonics at the DSV dissipate more rapidly with method B. A significant reduction of the residual gradient field is obtained using the design strategy B. It is known that there is a direct relationship between noise power from the cryostat vessel and power deposited as eddy currents. It may be the case that coils produced by method B cause more acoustic noise and heating of the cryostat than method A due to the increased intensity of ECs generated on the cryostat.

References: [1] Mansfield P and Chapman B. 1986, Journal of Magnetic Resonance; 66: 573-576 [2]- Peeren GN. 2003 Journal of Computational Physics;191:305–321 [3]-H. Sanchez, F. Liu, M. Poole and S. Crozier, submitted to ISMRM 2009.**Acknowledgements:** Financial support from the Australian Research Council is gratefully acknowledged.